RESEARCH ARTICLE | DECEMBER 13 2022

A flexible neutron spectrometer concept with a new ultra-high field steady-state vertical-bore magnet

Special Collection: New Science Opportunities at the Spallation Neutron Source Second Target Station

B. L. Winn ; C. Broholm; M. D. Bird ; B. Haberl ; G. E. Granroth ; J. Katsaras

Rev. Sci. Instrum. 93, 123903 (2022)
https://doi.org/10.1063/5.0122934

Review of Scientific Instruments ARTICLE scitation.org/journal/rsi

A flexible neutron spectrometer concept with a new ultra-high field steady-state vertical-bore magnet

Cite as: Rev. Sci. Instrum. 93, 123903 (2022); doi: 10.1063/5.0122934
Submitted: 26 August 2022 • Accepted: 14 November 2022 •
Published Online: 13 December 2022

B. L. Winn,[1,a)] C. Broholm,[2] M. D. Bird,[3] B. Haberl,[1] G. E. Granroth,[1] and J. Katsaras[1]

AFFILIATIONS

[1] Neutron Scattering Division, Oak Ridge National Laboratory, Oak Ridge, Tennessee 37830, USA
[2] Institute for Quantum Matter and Department of Physics and Astronomy, Johns Hopkins University, Baltimore, Maryland 21218, USA
[3] Magnet Science and Technology Division, National High Magnetic Field Laboratory, Tallahassee, Florida 32310, USA

Note: Paper published as part of the Special Topic on New Science Opportunities at the Spallation Neutron Source Second Target Station.
[a)] **Author to whom correspondence should be addressed:** winnbl@ornl.gov

ABSTRACT

The proposed facility explores materials under ultra-high magnetic fields. By combining the power of high fields to tune materials and of neutron scattering to probe the resulting changes down to the atomic scale, this facility will enable transformative progress in the study of quantum materials and is named for the "TITAN" subset of Greek gods to reflect this transformation. TITAN will offer DC magnetic fields up to at least 20 T. Exploiting the record brightness and bandwidth of the Second Target Station at the Spallation Neutron Source, TITAN will probe atomic-scale responses through high efficiency neutron spectroscopy up to 80 meV energy transfer, high resolution diffraction, and small angle neutron scattering. Focusing neutron optics will maximize flux on accurately positioned samples, while radial collimation and optimized shielding and detection strategies will minimize backgrounds.

I. INTRODUCTION

The transformative "TITAN" concept (a term from Greek mythology) is motivated by the alignment of a pressing scientific need and two exciting opportunities. The pressing scientific need is to provide extreme conditions,[1] and, in particular, high steady-state magnetic field,[2,3] in a way compatible with neutron scattering in order to reveal the atomic-scale structure and dynamics of quantum materials.[4] The first opportunity is the rapid advance of magnet technologies employing high temperature superconductors.[5] The second opportunity is found in the features of the Second Target Station (STS) to-be-built at Oak Ridge National Laboratory (ORNL) next to the existing First Target Station (FTS) of the Spallation Neutron Source (SNS). These features make it ideal for neutron scattering on samples under extreme and combined-extreme conditions, as described elsewhere.[6] These features include the unprecedented source brightness, the broadband moderators, and the large ratio of source period to neutron pulse duration.[7]

Concerning the pressing scientific need, there is tremendous excitement around the physics of quantum materials and their promise for a wide range of applications in energy and information technologies. The discovery that electronic topology profoundly impacts physical properties is enriching the field and bringing new understanding to previously intractable problems. A basic research needs workshop[4] defined priority research directions and resulted in considerable investments in quantum materials and quantum information. In 2018, Congress passed the National Quantum Initiative act, "To provide for a coordinated Federal program to accelerate quantum research and development for the economic and national security of the United States." Recently, DOE announced five National QIS Centers including the Quantum Science Center led by ORNL.

The overarching scientific challenge is to understand and control the quantum dynamics of strongly correlated electrons.[8] A quantum state of matter is characterized by its particular forms of emergent dynamics. An important class of experiments are those that can traverse distinct quantum phases within a single material and provide evidence for the associated transitions in the character of electronic quantum dynamics. Magnetic field is the ideal thermodynamic tuning parameter for quantum material studies.

Figure 1 illustrates a representative sampling of candidate materials with characteristic fields throughout a magnetic field continuum. Increasing the field available in split magnets for neutron scattering shows tremendous potential to broaden the scientific scope and impact of research. Indeed, SNS has recently increased the field available at the FTS's Hybrid Spectrometer (HYSPEC) from 8 to 14 T and has seen a dramatic increase in use and productivity. There are several systems shown for which it is known that fields in the range of 20–25 T would make a significant difference.

Other opportunities at other neutron scattering facilities have addressed this experimental need in the past. A different magnet technology and scatter geometry was employed to realize the High Field Magnet stationed at the Extreme Environment Diffractometer (EXED) at the research reactor BER II in Germany.[9] A different source and spectrometer strategy is implemented in the Extreme Environment Spectrometer BIFROST (a Norse mythological term from the region about the European Spallation Source) in Lund, Sweden, currently under construction.[10] What is proposed here implements different opportunities for both the magnet and the spectrometer, leading to unique capabilities for TITAN.

Concerning the first opportunity leveraged by TITAN, most steady-state magnets in use at neutron scattering facilities worldwide are based on vertical-bore split-coil magnets. Although this geometry represents a challenge in the magnet design, the advantages for scattering experiments are manifold. The same vertical sample rotation axis that preserves thermodynamic conditions at high fields provides optimal access to a circular disk of momentum transfer perpendicular to the field axis for neutron scattering. Established technologies for top loading inserts readily provide access to temperatures down to 50 mK, and the same liquid helium bath coil cooling strategy employed for vertical field split coil magnets for decades is compatible with recent advances in superconducting coils employing high temperature superconductor materials. This configuration also appears compatible with diamond anvil cells with a vertical axis, such as those developed at ORNL for inelastic neutron scattering[19] and single crystal diffraction.[20] These could be adapted for magnet compatibility with non-magnetic gaskets[6] (e.g., Russian alloy/NiCrAl) or for a small scattering aperture with null-scattering TiZr gaskets that could be used with polycrystalline diamond anvils, such as Versimax®. One could envision a scattering instrument designed for a horizontal bore magnet that would reach the highest magnetic fields and have a unique science program[21] as was implemented at EXED. The Titan concept avoids the severe limitations such a geometry places on TITAN's Quantum Materials focused neutron scattering scientific program.[22]

However, this split-coil geometry introduces intrinsic limits to the magnetic field at sample, compared to solenoid magnets. To date, high-field split magnets for neutron scattering have been constructed from the Low Temperature Superconducting (LTS) materials, NbTi and Nb_3Sn. While 23.5 T has been attained in LTS solenoids, the highest reliable field to date at the mid-plane of an LTS split magnet has been 15 T. This difference in central field is largely due to the fact that the maximum field on the conductor in a solenoid is only a fraction of a Tesla higher than that on the sample, while in a split magnet, the field on the conductor can be several Tesla higher than that on the sample. Consequently, a split magnet that provides 15 T to the user is operating around 20 T on the conductor, resulting in low critical current in the conductor and low coil-pack current density, large coils, etc. The pre-conceptual design of the 25 T split magnet described below has a peak field on the conductor approaching 35 T.

In the following sections, the technology proposed for the magnet is described first (Sec. II). The specific magnet configuration and compatible spectrometer concept are presented next (Sec. III). Simulation results of the instrument performance using realistic samples are then discussed (Sec. IV), followed by considerations and future work and refinements required (Sec. V).

II. MAGNET TECHNOLOGY

The so-called High Temperature Superconducting (HTS) materials were discovered in 1986. These materials, when operated at ~4 K, also superconduct at higher field than the LTS materials (>100 T vs ~25 T) and also have higher current densities at fields above ~15 T than the LTS materials do. These latter two properties make them excellent candidates for high field magnets. While people started building HTS test coils around 1990, the conductors used in these early test coils did not have uniform properties, were mechanically very weak, frequently required high-temperature reaction after winding with tight temperature and time windows,

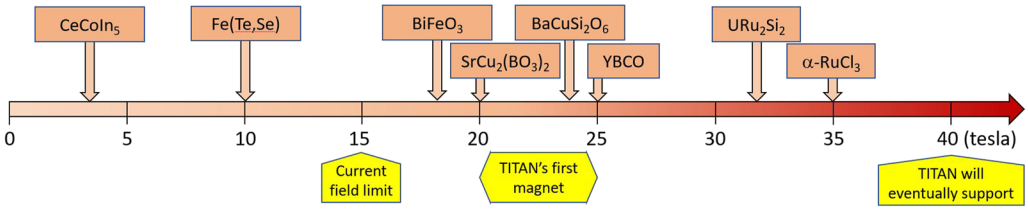

FIG. 1. Characteristic fields for various materials: $CeCoIn_5$,[11] Fe(Te,Se),[12] $BiFeO_3$,[13] $SrCu_2(BO_3)_2$,[14] $BaCuSi_2O_6$,[15] YBCO,[6,16] URu_2Si_2,[17] and α-$RuCl_3$.[18] The current world-wide steady-state vertical magnetic field limit for neutron spectroscopy is 15 T, as found, for example, at the Institut Laue-Langevin with the Cryomagnet 1580XHV26. At ORNL, the current maximum steady-state vertical field available is 14 T.

FIG. 2. A recent REBCO test coil at the MagLab that includes more advanced structural reinforcement and quench protection than the 32 T user magnet.

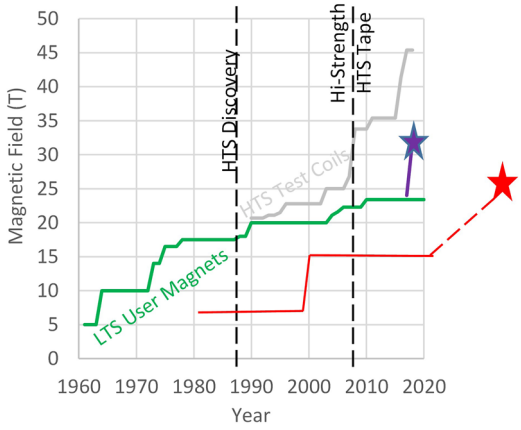

FIG. 3. Peak fields available worldwide from a variety of superconducting magnets. LTS solenoids (green), HTS solenoid test coils (gray), HTS user solenoids (purple), and split user magnets (red). By using the HTS technology similar to that used in the MagLab's 32 T solenoid, a split magnet for neutron scattering at a field >20 T should be feasible.

and were difficult to join. It was not until 2007 that a variety of HTS conductor with high strength and copper cladding was available fully reacted from the factory with reasonably uniform properties along its length. This conductor is based on a Rare Earth Barium Copper Oxide (REBCO) film and is frequently referred to as second generation HTS tape. It consists of a high-strength Hastelloy substrate strip (~50 μm) on which are deposited a few buffer layers to ensure grain alignment of the REBCO ($\ll$1 μm) followed by ~1 μm of REBCO, a Ag cap layer (~5 μm), and Cu cladding (~40 μm). There are presently several suppliers of various versions of this material worldwide.

In 2007, SuperPower developed a high-strength REBCO tape and built a test coil that was tested at the National High Magnetic Field Lab (MagLab) in Tallahassee, Florida. The REBCO coil was installed in the bore of a 20 T resistive magnet and energized to 7 T, providing a total field of 27 T, a world record for an HTS test coil at the time. A number of test coils using REBCO have been built since that time (see, for example, Fig. 2) with the highest field attained to date being 45 T, also at the MagLab (gray trace shown in Fig. 3).

Based on the success of various REBCO test coils in the 2007–2008 timeframe, the MagLab submitted a proposal in early 2009 to the National Science Foundation to build a 32 T all-superconducting general-purpose magnet for condensed matter physics. The magnet reached field in 2017 and is now serving users at fields up to 32 T (purple trace in Fig. 3). Bruker Biospin has also used the REBCO tape to build nuclear magnetic resonance (NMR) magnets up to 1.2 GHz (28.2 T). At least two organizations are developing NMR magnets up to 1.3 GHz (30.5 T), and several organizations worldwide are now developing condensed matter physics magnets with goals of 30 T or more. The highest targeted field presently is the 40 T system being developed by the MagLab.

In recent years, tremendous progress has been made in REBCO magnet technology to provide consistent, reliable quench protection, to understand the effects of screening currents in the broad tape (~4 × 0.001 mm^2), and to understand the fatigue performance of the tapes and coils. A number of commercial magnet firms now see the market for HTS magnets in the 25 T range to be large enough to justify development of such products.

As shown in Fig. 3, the fields available from high field solenoids are increasing. The time is right to push facilities for neutron scattering beyond the 15 T limit that has been in place for 20 years (red trace). The HTS magnet technology opportunity for TITAN is to replace that part of the coils that needs to remain superconducting in the presence of higher magnetic fields than the LTS conductors afford. However, to realize this in robust, functional solenoid magnets has required significant research and development. For split coils, some work has already been done, as described below. Further research and development is required to address aspects of split magnets, such as gap-side connections, that do not exist in solenoids.

Some initial work on split magnets has been undertaken. The Department of Energy has funded some work via the Small Business Innovation Research (SBIR) and Small Business Technology Transfer (STTR) programs. One project included a grant to Energy to Power Solutions (e2P) to build a small split pair of coils that was then delivered to the MagLab to be installed in a 12 T large-bore superconducting magnet and energized. A Mechanical Test System (MTS) was used to apply axial compression to the REBCO coils to simulate the compression that would be experienced by full-scale coils. The REBCO coils were compressed 600 times to 10 kN and an additional 500 cycles to 20 kN without significant degradation. This was one of the first tests worldwide of REBCO coils with high currents and high axial compression simultaneously.

A design study at the MagLab was performed to evaluate the pre-conceptual design of a 20–25 T vertical field split magnet suitable for use in neutron scattering, specifically for use at the STS. This effort started with the conceptual design of a 40 T solenoid

mentioned above and removed the conductor from the mid-plane and replaced it with structural material and vacuum space for scattering. The Lorentz forces between the two halves of the coils was computed and the stress in the structural spacer was computed. The spacer and coils were redesigned. By adjusting the relative lengths of the coils, the clamping pressure on the spacer can be adjusted. By increasing the thickness of the spacer, its strength can be increased at the expense of the central field. A converged solution was found for each of two different versions: one with elliptical scattering ports and the other with rectangular ports. As expected, the rectangular ports result in larger stress concentrations and more structural reinforcement that results in lower central field than in the version with elliptical ports. However, the rectangular ports provide more solid angle for scattering.

Building a split magnet will require novel features compared with a solenoid, which require further development. In particular, making electrical terminations on REBCO coils typically requires a lot of space. Doing so near the mid-plane of a split magnet will require some development due to the inherent space constraints. The next step toward realizing such a magnet would be to build split test coils to be tested to high current, stress, and field inside a large bore solenoid to verify that these novel features perform as intended prior to committing to real user magnet.

In addition, another HTS magnet technology has been in development at the MagLab. $Bi_2Sr_2CaCu_2O_{8+x}$ (Bi-2212) wire is round, which makes coil winding much easier than with the broad REBCO tape. However, it also requires a high-temperature reaction after winding to create the superconductor. It also has very low mechanical strength. Consequently, for many years, the current density achievable in Bi-2212 coils was significantly lower than that available from REBCO coils, which means that to realize a magnet of a particular field value, the REBCO magnet would be smaller than the Bi-2212 magnet. For this reason, most magnet groups over the past fifteen years have focused on REBCO. However, recent advances in Bi-2212 conductor fabrication[23] point to a competitive alternative for next generation dipoles and quadrupoles. Extensive work has been undertaken to improve the quality of the powder from which the wire is made and the reaction process that converts the raw wire into a superconductor. These have resulted in dramatic improvements in critical current density in the wires. In addition, work on coil fabrication and reinforcement have led to test coils with high overall current density as well. This coil technology also is showing promise for future vertical field split magnets in the 20–25 T range.

III. MAGNET AND SPECTROMETER CONCEPT

The 20–25 T uncompensated magnet concept for TITAN has the following specifications. The cold-bore inner vacuum chamber inner diameter is 35 mm to accommodate ultra-low temperature inserts and moderate pressure diamond anvil cells[20,24] (e.g., <15 GPa on a 0.5 mm^3 sample or <10 GPa on a 1 mm^3 sample), the mid-plate gap is 10 mm with an additional 2 mm for cadmium shielding, and vertical divergence is ±5° out of the horizontal plane. The magnet employs a wedge support strategy at the gap as opposed to concentric aluminum ring supports because for time-of-flight based measurements, multiple scattering effects from such support structures yield time-dependent background, which introduce spurious features at different wavelengths for elastic measurements and at various energy transfers for inelastic measurements. Eight openings between wedge supports shall be equally spaced, with 6 openings 25° wide and the incident and downstream openings 26.5° wide. To establish continuous horizontal scatter angle coverage, this magnet shall be rotated to reorient the wedge openings.

The instrument design described here is revised relative to the original TITAN proposal, which also accommodated further separate extreme environments and environmental combinations to push the limits on high pressure, high temperature, and multi-extremes. The ambitious concept that resulted from including additional sample area requirements and scatter geometries made TITAN as proposed prohibitively expensive. Therefore, based on recommendations from a concept review process for the STS project, the concept was scaled back so the scatter geometry matches to the magnet geometry. Nonetheless, even the current design will enable multi-extreme conditions by combining the vertical magnetic field with temperature from 50 mK to 400 K and a pressure of 10–15 GPa for spectroscopy on select materials.

A 25 T magnetic field imposes a natural energy scale that must be matched to the instrument design. The Zeeman energy is $g\mu BS{\cdot}B$; considering g = 2 and spin quantum numbers $1/2 < S < 3$ with the Bohr magneton value of $\mu B = 0.058$ meV/T, a 25 T magnetic field amounts to an energy scale between 2 and 8 meV. The optimized high brightness of the STS cold moderators in this energy range makes STS the source of choice for TITAN.

TITAN will be designed to employ direct geometry spectroscopy (DGS). Compared to indirect geometry spectroscopy (IGS), DGS accesses more of the high energy transfer/low momentum transfer regime, which is important to probe the magnetism of quantum materials, due to the restriction of final energies below 5 meV. DGS also provides more access to low-energy transfers at high momentum transfer and access to large neutron energy gain processes (see Fig. 4). DGS is also more easily scalable to increasing solid angle by choosing taller ^{3}He linear position-sensitive detector tubes. For TITAN, an increased vertical divergence better matches to the magnet's proposed ±5° out of the horizontal plane, compared to BIFROST,[10] which is constrained to ±2.3° to ±3° depending on the final energy due to the high cost of the pyrolitic graphite analyzer crystals and the large area associated with this coverage. DGS preserves out-of-plane resolution via position sensitive detectors, unlike the multiplexed IGS approach. Finally, DGS shares a common final flight path and detector geometry with wide-bandwidth diffraction and small angle neutron scattering (SANS). Therefore, all these techniques can be combined in one instrument with minimal compromise.

The uncompensated high field magnet imposes significant instrument design constraints. First, the sample region shall accommodate up to 2 m diameter, both for the first-generation magnet with an uncertain outer diameter and for subsequent magnets as higher field systems become achievable, up to 40 T at sample. This sample region shall be floor mounted to facilitate the needed magnet rotation, which enables continuous horizontal angle coverage with only two orientations of the magnet. Design of nearby choppers, detectors, and electronics shall be by design and via testing verification operationally robust in anticipated stray fields, and no ferromagnetic material shall be near the sample position. In addition, both detectors and choppers need to be in sufficiently low field environments by physical distancing and/or shielding. The nearby

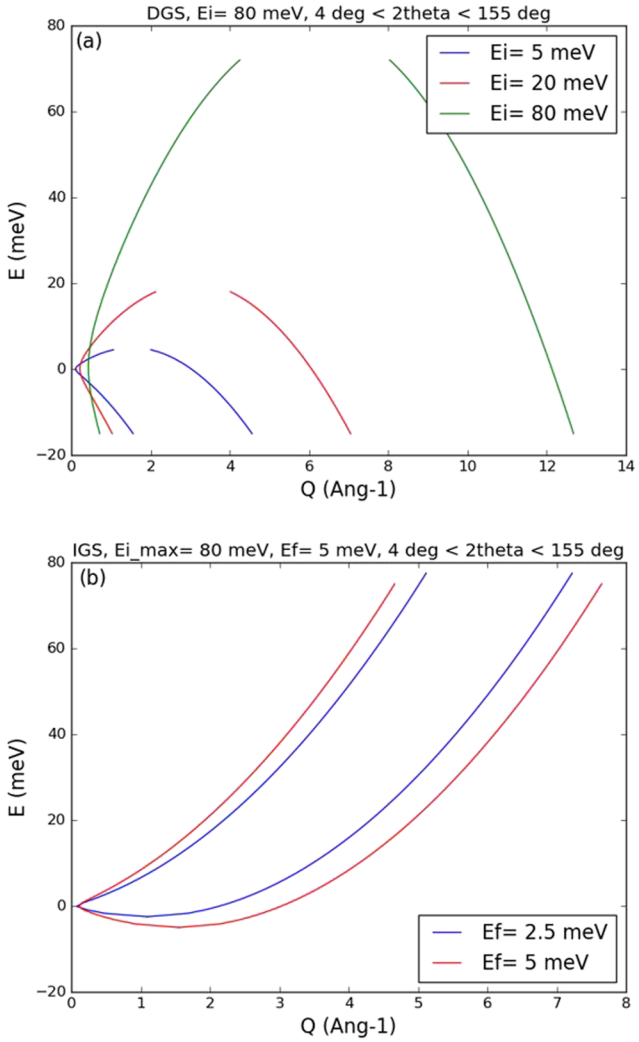

FIG. 4. Momentum and energy transfer range with a maximum incident energy of 80 meV for both (a) direct and (b) indirect geometry spectroscopy with the final energy below the 5 meV beryllium filter cutoff. For DGS, (a) neutron energy gain continues to large negative values only constrained by the ^{3}He detection efficiency.

space shall be allocated for dedicated helium recovery and recondensation, quench protection, and dilution refrigeration infrastructure for sample cooling. Finally, the scatter geometry shall match that of the magnet with only ±5° out of the horizontal plane.

Therefore, the sample region must be physically removed from other instrument end-stations. One feature valuable to the STS or any new facility is the ability to strategically map beamlines out, which proves particularly useful to accommodate the unique demands of TITAN. The proposed location is beamline 2, with 55 m between the moderator and sample. Beamline 2 is on the "short" side of the STS, facing the FTS. The 55 m distance places the high field magnet sufficiently far from neighboring instruments and the STS mezzanine so the uncompensated and unshielded stray field is below the 5 Gauss OSHA limit at these locations.

Beginning with careful prioritization under these well-defined constraints and using sound predictive analytical models and engineering solutions to move beyond conventional intuition for optimizing spectroscopy, an excellent solution has been found, which now serves as a starting point for future refinement. One equation,[25,26] which relates relative energy resolution at the elastic line to instrument geometry, is particularly useful for DGS optimization,

$$\left(\frac{\Delta E}{E}\right)^2 = \left(\frac{2v(L_2+L_3)\Delta t_s}{L_1 L_3}\right)^2 + \left(\frac{2v(L_1+L_2+L_3)\Delta t_m}{L_1 L_3}\right)^2 + \left(\frac{2\Delta d_D}{L_3}\right)^2. \quad (1)$$

The variables in this expression are defined in Table I. The scientific focus of TITAN and past experience indicate targeting a range of $2\% < \Delta E/E < 5\%$ at the elastic line for spectroscopy.

The next major consideration is to determine the time profile of the "source" Δt_s. For direct geometry spectroscopy, the source may be established either at the moderator itself or via a fast burst chopper well upstream of the monochromating chopper known as the "P" chopper. The STS offers two different kinds of liquid hydrogen moderators, the "cylinder" and the "tube," where the "cylinder" has a shorter time profile due to a shorter depth along the incident beam direction.[7,27] The "tube" moderator is employed for STS's Chopper Spectrometer Examining Small Samples (CHESS), which is a DGS,[28] so that they may use the broader time structure to optimize the use of both "P" chopper and the monochromating chopper to enable repetition rate multiplication for a set of fixed incident energies while maximizing flux at each energy by leveraging the plateau region of the "tube" time profile for a range of energies. The TITAN instrument instead forgoes the "P" chopper and leverages the time structure of the "cylinder" moderator for several reasons. With the moderator to sample distance already set at 55 m, the primary spectrometer dimension $L_1 + L_2 = 55$ m is longer than FTS's HYSPEC DGS,[29] which achieves the target energy resolution range even with a long L_2, which has proven advantageous for operation with uncompensated magnets already. By setting the time-burst at the moderator, for repetition rate multiplication, TITAN can continuously adjust the set of incident energies, despite the energy-dependent delay of the peak moderated flux compared to the pulsed spallation events producing high-energy neutrons. The STS cylinder moderator enables DGS spectroscopy with E_i's up to 80 meV with reasonable brightness and pulse widths, which vary from 9 μs

TABLE I. The principal parameters defining the energy resolution of a direct geometry neutron spectrometer through Eq. (1).

$\Delta E/E$	Relative energy resolution (FWHM)
L_1	Distance from "source" to monochromating chopper
L_2	Distance from monochromating chopper to sample
L_3	Distance from sample to detector
v	Speed of the neutron at energy E
Δt_s	Time profile of the "source" (FWHM)
Δt_m	Time profile of the monochromating chopper (FWHM)
Δd_D	Uncertainty in distance from scattering to detection (FWHM)

at 80 meV to 154 μs at 2 meV; see Fig. 5 of Ref. 27 and the description of both moderators found in the same. There are no plans for a solid methane moderator[30] at STS, but such a moderator would provide a shorter Δt_s at low incident energies.

The energy resolution is also determined by Δt_m, which when leveraging a 300 Hz double disk chopper determines maximum beam-size requirements for a virtual source at the monochromating chopper to 18 × 18 mm^2 to obtain a minimum of 15 μs burst time. By setting L_2 = 6 m and L_3 to a minimum of 4.5 m, the target energy resolution was achieved [see Fig. 5(b)]. By restricting L_3 to a maximum of 6.5 m, repetition rate multiplication is operable over nearly all configurations. This L_2 is similar to what was proposed earlier[21] and further than either the HYSPEC chopper or the EXED chopper[31] in order to conservatively accommodate magnetic bearings for the chopper in the presence of the magnet's stray field and to accommodate even higher stray-field magnets in the future. In the current design, L_3 = 4.5 m for scatter angles between −155° and +155°, except for the horizontal scatter angle range −4° to +6° where L_3 = 6.5 m to enable SANS. Following the strategy of Ehlers *et al.*,[26] we note that for the contributions to elastic energy resolution to be comparable, one can equate the first two terms in Eq. (1) and determine a ratio between Δt_m and Δt_s, and with the proposed primary configuration (L_3 = 4.5 m), this ratio is

$$\frac{L_1 + L_2 + L_3}{L_2 + L_3} = \frac{59.5\ \text{m}}{10.5\ \text{m}} = 5.67 \tag{2}$$

so that even burst times of 15 μs can impact energy resolution.

There is a way to transform a high performing spectrometer with a single configuration change into a high performing wide bandwidth diffractometer and/or small angle neutron scattering instrument. Many DGSs already employ a broadband time of flight diffractometer configuration that is functional, if not optimal, to quickly evaluate single crystal orientation via Laue diffraction at the beginning of experiments. This is achieved by removing or stopping at the open position of the monochromating chopper and optionally the "P" chopper. To optimize also for elastic scattering, it is useful to consider the momentum resolution for elastic scattering as a function of $L = L_1 + L_2 + L_3$, Δt_s, and scatter angle 2θ as follows:

$$\left(\frac{\Delta Q}{Q}\right)^2 = \left(\frac{\Delta t_s}{t}\right)^2 + \left(\frac{\Delta L}{L}\right)^2 + (\cot\theta\Delta\theta)^2. \tag{3}$$

The "cylinder" moderator, which was chosen because of the long incident beam flight path, is also the best choice for high Q resolution with its low $\Delta t_s/t_s$ compared to the tube moderator. That, combined with L > 55 m, causes $\Delta Q/Q$ to be driven primarily by cot $\theta\Delta\theta$. While for DGS L_3 is bounded by energy resolution requirements as a lower bound and repetition rate multiplication as an upper bound, the angle resolution $\Delta\theta$ is partially determined by both $L_3(2\theta)$ and detector pixel size $d(2\theta)$ via $\Delta\theta = L_3/2d$. The detector pixel size $d(2\theta)$, in turn, can be at or larger than the characteristic sample size, which for the TITAN magnet is set to a maximum of 1 cm, although finer pixelation may prove advantageous to reduce the relative "background" associated with spin-incoherent or isotope-incoherent scattering for smaller samples. Although incident neutron beam acceptance and sample mosaic also contribute to $\Delta\theta$, they may be partly mitigated via super-resolution/deconvolution

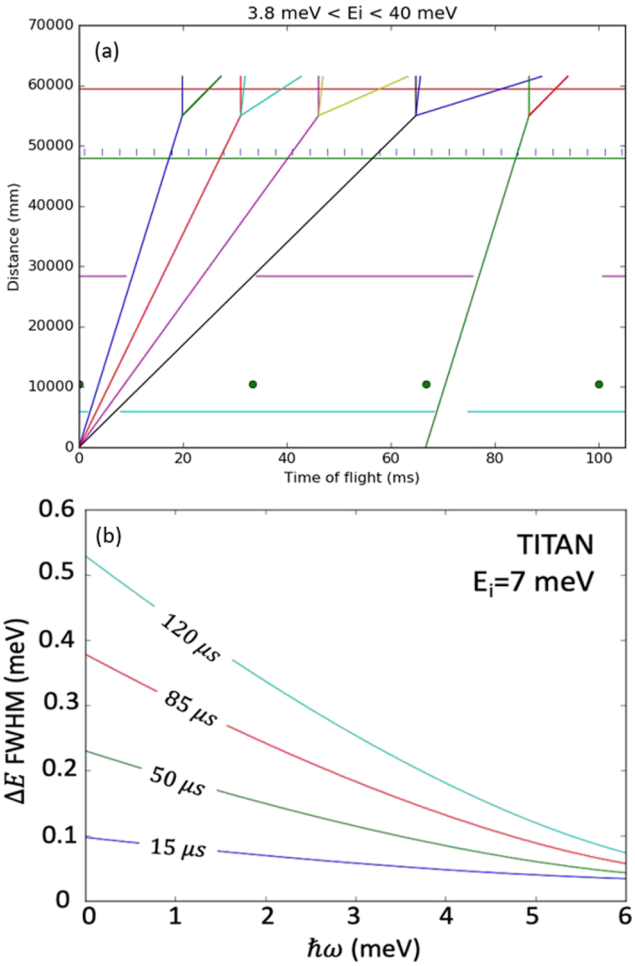

FIG. 5. (a) Time-of-flight diagram illustrating repetition rate multiplication with DGS. The vertical blue lines indicate the 300 Hz monochromating chopper opening at 15 μs, the vertices indicate the location of the sample, and the top red line indicates the L_3 = 4.5 m position and the trajectories ending at the L_3 = 6.5 m position. The green circles represent the T0 chopper, the magenta horizontal lines represent the two bandwidth choppers, the cyan lines represent the frame overlap choppers, and the green horizontal line represents the two repetition rate multiplication selector choppers. (b) Energy resolution expressed as full width half maximum (FWHM) as a function of energy transfer for a range of chopper burst times between 15 and 120 μs for E_i = 7 meV, where Δt_s = 93 μs.

strategies so long as detector pixelation is sufficiently fine. Resolution requirements for SANS for quantum materials are less than that for other systems, at $\Delta Q/Q$ ~ 4%, while for diffraction, the desired resolution is $\Delta Q/Q$ ~ 0.4%. Assuming L_3 = 6.5 m for SANS and 2θ ~ 2°, then a ^{3}He detector tube diameter of 8 mm is sufficient, while assuming L_3 = 4.5 m for diffraction and 2θ ~ 40°, then a ^{3}He detector tube diameter of 12 mm is sufficient. Therefore, by selecting the right combination of L_1, L_2, $L_3(2\theta)$, and $d(2\theta)$ to establish both DGS energy resolution and elastic Q resolution, spectroscopy, SANS, and diffraction all become powerful scattering techniques for the experimental applications envisioned for one-of-a-kind stationary magnet at TITAN. Scattering technique flexibility is valuable with

such a unique magnet because while studies of quantum materials also benefit from SANS and diffraction, the magnet cannot operate at any other instrument besides TITAN. Further optimization may vary the radial distance in a more continuous fashion to better optimize Q resolution.

The 15 Hz STS spallation frequency enables several energies for rep-rate multiplication or reasonable bandwidth for ToF diffraction and SANS, despite $L_1 + L_2 = 55$ mm. A direct consequence is restriction to ~4 Å bandwidth at 15 Hz and ~8 Å bandwidth at 7.5 Hz for wide-bandwidth diffraction. The 7.5 Hz operation is achieved via occlusion of alternating pulses and slowing the bandwidth choppers. Both resolution at $E_i = 7$ meV and repetition rate multiplication for an example set of E_i's are illustrated in Fig. 5(a).

For structural refinement at high fields, diffraction with an extended wavelength range down to 0.64 Å (200 meV) is needed, and this motivates two other features of TITAN. With the cold "cylinder" moderator, there are few neutrons at 200 meV but enough to be used for white beam diffraction measurements. This will enable full structure analysis and pair distribution function analysis at high fields. Therefore, TITAN shall employ a direct line-of-sight between the moderator and sample and a T0 chopper, which accommodates this wavelength. Assuming that the T0 chopper is located within the bunker, this chopper must operate at 30 Hz instead of the STS 15 Hz spallation repetition rate. The resulting high-level geometry for TITAN is summarized in Table II, and a rendering of the design concept is shown in Fig. 6.

The inclusion of SANS, along with the need for continuous scatter angle coverage, introduces separate technical challenges. To remain flexible at the sample region while preserving continuous coverage, sapphire windows[32] are employed for entry into an evacuated flight path beyond the 2 m diameter sample region, instead of implementing a fully evacuated path between magnet and detector. In addition, for SANS, the last 6 m of focusing optics before the sample is removable to reduce the divergence at 4 Å from 2° to 0.2°, with further reduction in divergence achievable via the aperture system at the monochromating chopper. In all cases, L_2 shall be primarily in vacuum, except for a narrow section before the magnet.

TABLE II. High level geometry for TITAN.

DGS geometry	(m)	Cross section	(cm^2)
L_1	49	Moderator	3 × 3
L_2	6	M-chopper aperture	1.8 × 1.8
L_3	4.5	Sample-large	1 × 1
L_3-small angle	6.5	Sample-small	0.1 × 0.1
Chopper location	**(m)**	**Scatter geom.**	**(°)**
Frame overlap	6	Left banks, h.	6–155
T0	10.5	SANS banks, h.	−4 to 6
Bandwidth	28.5	Right banks, h.	−4 to −155
Rep-rate sel.	48	Out of plane	±5
Monochromating	49		

The combination of the STS cylinder moderator's small square profile of 3 × 3 cm^2 and state-of-art ballistic focusing optics enables high brightness and brightness transfer. The guide system provides a focus at the monochromating chopper and optionally at the sample via four-walled elliptical guides. The profile for the first ellipsoidal section is square to match the moderator profile, while some options for the second ellipsoidal section may be changed asymmetric to match expected sample dimensions. Eliminating the "P" chopper has

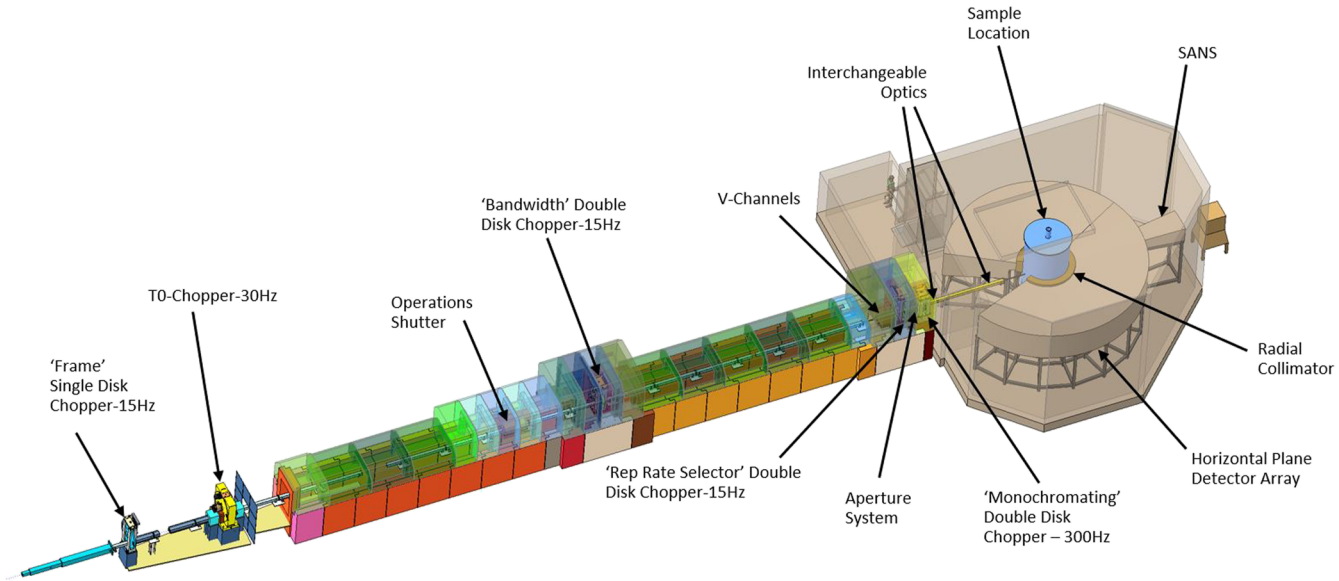

FIG. 6. Overview of entire spectrometer. Chopper frequencies are noted in the labels.

TABLE III. The ballistic guide geometry parameters used for initial simulations. The short axis half width for the ellipse profile is *b*, while the focus is *c*.

	Ellipse (m)			Section (m)	
	b	*c*	Center	Start	Stop
L_1	0.038	25.3	24.25	0.98	48.8
$L_{2\ \text{large}}$	0.013	3.6	51.4	49.2	54.5
$L_{2\ \text{small}}$	0.007	3	52	49.2	54.9
	Ap. cross section (m)			Ap. location (m)	
$L_{2\ \text{SANS}}$	0.01	0.01		49	54

the bonus of reducing the number of foci required, which improves low wavelength brightness transfer with both fewer and on average more shallow reflections. For SANS, the focusing optics along L_2 is replaced by an evacuated flight tube. Similarly, for sample sizes at or under 1 mm characteristic dimension, the optics along L_2 shall be replaced to provide a smaller focal spot size for improved signal-to-background as well as modestly increased divergence to trade-off between signal and ΔQ, and with $L_2 = 6$ m, this small-sample optics has the added advantage of sufficient distance for effective ballistic focusing.

Details of the guide system geometry used for simulations are found in Table III. The vertical and horizontal profiles were the same, and the cross section is square. Neither choppers nor guide gaps and windows were simulated for any but the monochromating chopper, and magnet interference was ignored. All guides were presumed to have $m = 6$.

Further guide model studies are needed to determine whether a smaller focus at the monochromating chopper than required for the desired energy resolution may provide better brightness transfer. Additional optimization shall be needed to refine the three different optics configurations between the monochromating chopper and the sample position to increase both intensity and acceptance for smaller samples (the two are coupled via Liouville's theorem when employing reflective optics) and to account for samples with differing heights and widths. One alternative to continuous single walled ballistic guides along L_3 is to employ nested mirror optics with interchangeable collimators to more discretely adjust the beam size and to move the focusing optics further away from the magnet[33] or to explore focusing at detectors for the SANS configuration.[34] Another alternative is to sacrifice the high energy neutrons for the smallest samples and leverage the SELENE concept[35] (named for the Titan goddess of the moon due to the similarity of the focusing optics curvature to the light-to-shadow border on the moon) proposed for the BIFROST instrument at the European Spallation Source.

IV. SIMULATION RESULTS FOR THE TITAN CONCEPT

Simulations of the TITAN instrument demonstrate its power as both a rep-rate DGS and as a diffractometer. Simulations were performed with a slightly modified scatter geometry with an out of plane acceptance of ±7° instead of the newly proposed ±5° and in the horizontal plane from −155° to +110° instead of through +155°. Simulations employed both the Monte-Carlo Simulation Triple Axis Spectrometer (McStas) simulation package for the beamline[36] and

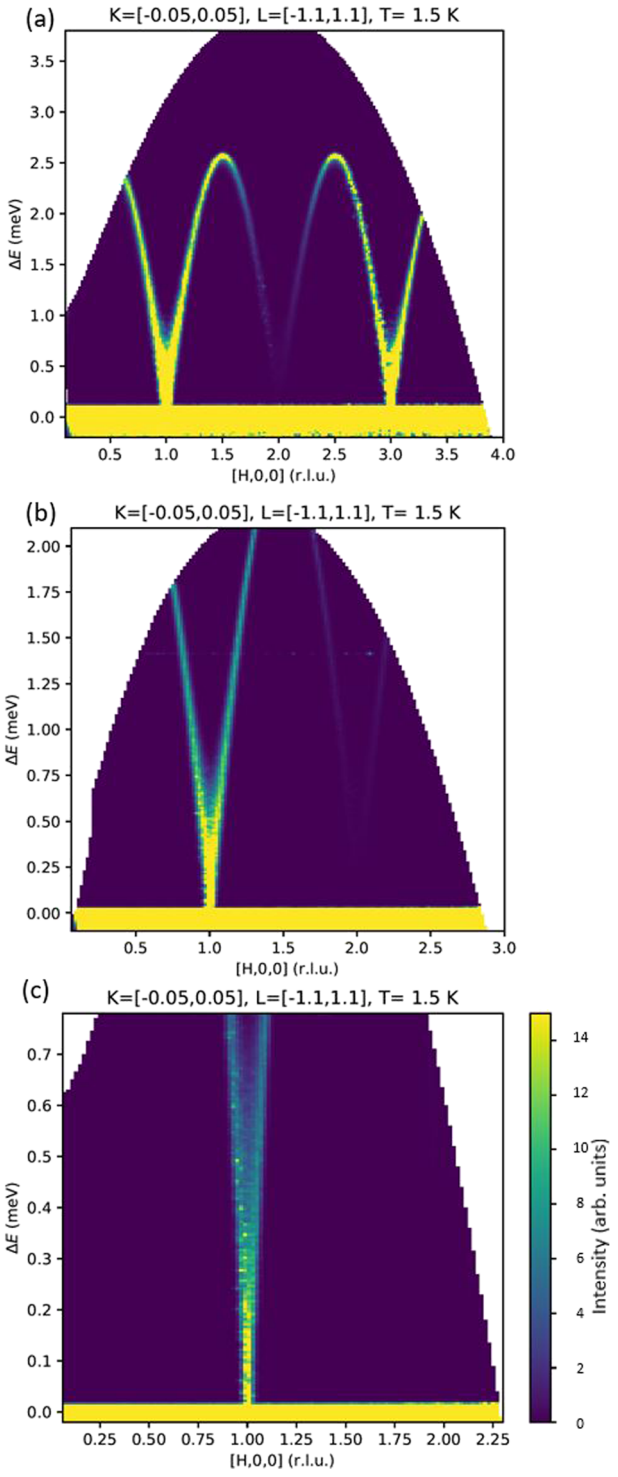

FIG. 7. Spin wave simulations for $K_2V_3O_8$ at incident energies 4.0 meV (a), 2.38 meV (b), and 1.45 meV (c) as in the rep-rate multiplication configuration indicated in Fig. 5. For a 1 g sample, 4 h is needed for a complete measurement (8 settings, 2° steps, and 2 magnet orientations, integrated over all *L*) of the 2D magnetic excitation spectrum. Simulated results using McStas and McVine.

the Monte Carlo Virtual Neutron Experiment (McVine) sample kernel package.[37] The Monte Carlo data were reduced using the Mantid software,[38] as intended for the operating instrument.

A scientifically meaningful range of incident energies enable inelastic magnetic scattering from a 2D quantum magnet in 4 h for a 1 g sample (Fig. 7). This simulation provides a benchmark relevant to experiments probing quantum magnetic materials at high magnetic fields. The simulation also demonstrates the power of repetition rate multiplication to expose a broad dynamic range of excitations with high efficiency, which will be important experiments on small crystals driven to criticality by high fields and/or pressure. Likewise, single crystal diffraction from a 1 × 1 mm^2 beam yields a full diffraction pattern in a single setting of the sample after 40 min (Fig. 8). This sample with this beam profile is simulated to illustrate the performance of the white beam diffraction mode of operation.

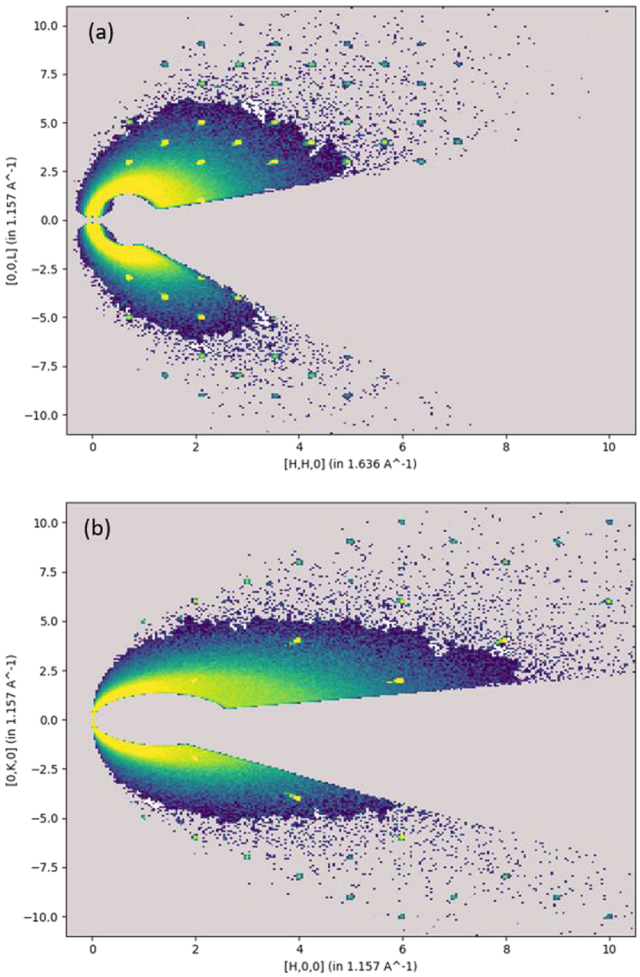

FIG. 8. Broadband diffraction of a single crystal of silicon shaped as an annulus, 4 mm tall, 6 mm diameter, and 1 mm wall thickness. Each image represents a different orientation of the sample [(a) in the HHL plane and (b) in the HK0 plane] and an acquisition of 40 min (20 min each for two magnet orientations). The bandwidth employed for this simulation is in the brightest region of TITAN's spectrum from 2 to 9 Å. This entire spectrum may be employed simultaneously using 7.5 Hz operation with an 8 Å bandwidth. Simulated results using McStas and McVine using an acquisition time of 20 min.

V. DISCUSSION AND CONCLUSION

While the concept described here promises many new research avenues for quantum materials research, further development is needed for TITAN. First and foremost, a concerted research and development program is proposed to advance the technical readiness of split-coil HTS technology. In addition, further concept development is needed in the gap wedge design to minimize stress while preserving as much scatter solid angle as possible via modest radiusing to mitigate stresses at otherwise sharp corners or via a hybrid approach with both wedges and alumina support rings. These studies may be performed using existing coil models and forces and with McVine simulations to evaluate and minimize multiple scattering. Both active compensation and passive shielding of the magnet and of field sensitive equipment, such as the monochromating chopper, need to be explored further. Active compensation has proven useful not only for reducing stray field but also for improving compatibility with nearby polarization filtering components. However, it does increase the complexity, diameter, and cost of the magnet system. Finally, while the current concept employs a 35 mm inner diameter for the cold-bore sample volume to preserve compatibility with ultra-low-temperature inserts, more studies are needed to better understand how the maximum field-at-sample changes as the current 12 mm sample gap is reduced while increasing inner diameter toward 50 mm to become better compatible with either higher pressure diamond anvil cells or high temperature inserts.

The TITAN instrument concept itself also needs further refinement. Continuous variation of L_3 and further optimization of the guide systems have already been mentioned. The simulation shown in Fig. 7 represents a simplified chopper geometry with only one incident energy simulated at a time. The full chopper complement needs to be modeled to verify the estimated frame overlap suppression and proposed routes to optimize chopper opening times for different energies. This full simulation is expected to demonstrate the asymmetric effect on energy resolution due to the "Ikeda-Carpenter tail"[39] and sharp leading edge of the moderated neutrons for the cylinder moderator, and options via additional choppers to mitigate those features for at least one E_i need to be explored.

Careful accounting of the magnet's stray field is needed to ensure safe and robust operation of TITAN. The stray fields need to be modeled not just for the first-generation magnet but also extrapolated to accommodate steady state magnets with field at sample of up to 40 T. With this stray field profile, the region around the sample position can be better optimized with nonmagnetic materials and with a design that minimizes eddy currents during a quench. In addition, these stray fields shall be used to design appropriate magnetic shield for choppers. It is anticipated that some motion control systems may require physical removal of the electromagnetic motors themselves and instead employ shafts and gears to manipulate systems in the region around the magnet.

Development on instrument relevant technologies is required. The maximum detector tube lengths, which enable robust operation

for various tube diameters, still needs to be determined. The adoption of the tube-array on vacuum flange strategy, which has been successfully implemented at the High Resolution Chopper Spectrometer (HRC) at the Materials and Life Science Experimental Facility (MLF) of the Japan Proton Accelerator Research Complex (J-PARC),[40] promises to vastly simplify maintenance of the detector system but needs in-house testing and vetting. The goal of providing continuous coverage through small scatter angles with adequate resolution and coverage, while reducing the effects of small angle scattering, shall be achieved via sapphire windows, but the panel frame design requires optimization to minimize occlusion between windows.

With a focus on a dedicated split coil steady-state magnet and direct geometry spectroscopy, TITAN can bring a full range of powerful neutron scattering techniques to the exploration of quantum materials at ultra-high magnetic fields. The richness of this scientific area has been recognized for decades, but an instrument like TITAN is only now becoming feasible due to advances in HTS magnet technologies and the unique capabilities afforded by the Second Target Station. To make this transformative instrument available for day one experiments at the STS, a steady R&D program outlined in this article needs to be initiated immediately.

ACKNOWLEDGMENTS

The authors thank all the members of the TITAN proposal team, who worked diligently from the fall of 2020 to the summer of 2021 to prepare an ambitious and innovative facility concept for prototype extreme environments leveraging the STS. Takeshi Egami (University of Tennessee), Sergey Ushakov (Arizona State University), and Dante Quirinale (ORNL) comprised the high temperature advocates for TITAN. Chen Li (University of California, Riverside), Stan Tozer (National High Magnetic Field Laboratory, Florida State University), coauthor Bianca Haberl, and Yan Wu (ORNL) provided high-pressure advocacy. Mu-Ping Nieh (University of Connecticut) and co-author John Katsaras (ORNL) provided soft mater and biological extreme condition advocacy. Hiroyuki Nojiri (Tohoku University), John Singleton (National High Magnetic Field Laboratory, Los Alamos National Laboratory), co-author Garrett Granroth, and Masa Matsuda (ORNL) provided pulsed magnet advocacy. Despite the transition back to a steady-state magnet centered concept, these team members were also kind enough to provide constructive feedback on this publication. These unique and profoundly insightful extreme environment developers and advocates have transformed the way that the authors approach the development of instrument design concepts from the perspective of extreme environment prototyping needs.

Thanks to Gabriele Sala (also a member of the TITAN proposal team), Christina Boone, Jiao Lin, and other STS project staff who provided simulation results (Figs. 4 and 5) and engineering support for this paper, which represents only a small fraction of the support they provided for preparation of the TITAN concept and proposal. Thanks to Jack Toth, Dylan Kolb-Bond, and Scott Bole (MagLab, Florida State University) who performed the structural optimization, magnetic optimization, and mechanical design of the split magnet.

This research used resources of the Spallation Neutron Source Second Target Station (SNS STS) Project at the Oak Ridge National Laboratory (ORNL). ORNL is managed by UT-Battelle LLC for DOE's Office of Science, the single largest supporter of basic research in the physical sciences in the United States. The design study performed by MagLab was funded by the SNS STS Project. Barry Winn, Bianca Haberl, Garrett Granroth, and John Katsaras acknowledge the support of the Department of Energy, Basic Energy Sciences, Scientific User Facilities Division. This manuscript was authored by UT-Battelle, LLC, under Contract No. DE-AC05-00OR22725 with the U.S. Department of Energy. The United States Government retains and the publisher, by accepting the article for publication, acknowledges that the United States Government retains a non-exclusive, paid-up, irrevocable, world-wide license to publish or reproduce the published form of this manuscript, or allow others to do so, for United States Government purposes. The Department of Energy will provide public access to these results of federally sponsored research in accordance with the DOE Public Access Plan (http://energy.gov/downloads/doe-public-access-plan).

AUTHOR DECLARATIONS

Conflict of Interest

The authors have no conflicts to disclose.

Ethics Approval

Ethics approval for experiments reported in the submitted manuscript on animal or human subjects was granted.

Author Contributions

B. L. Winn: Conceptualization (equal); Formal analysis (equal); Methodology (equal); Writing – original draft (equal). **C. Broholm**: Conceptualization (equal); Methodology (equal); Writing – original draft (equal); Writing – review & editing (equal). **M. D. Bird**: Methodology (equal); Writing – original draft (equal); Writing – review & editing (equal). **B. Haberl**: Conceptualization (equal); Methodology (equal); Writing – original draft (equal); Writing – review & editing (equal). **G. E. Granroth**: Methodology (equal); Writing – review & editing (equal). **J. Katsaras**: Conceptualization (equal); Writing – review & editing (equal).

DATA AVAILABILITY

The data that support the findings of this study are available from the corresponding author upon reasonable request.

REFERENCES

[1] J. Wadsworth, G. W. Crabtree, R. J. Hemley, R. Falcone, I. Robertson, J. Stringer, P. Tortorelli, G. T. Gray, M. Nicol, J. Lehr, S. W. Tozer, T. Diaz de la Rubia, T. Fitzsimmons, J. S. Vetrano, C. L. Ashton, S. Kitts, C. Landson, B. Campbell, G. Gruzalski, and D. Stevens, "*Basic research needs for materials under extreme environments.* Report of the basic energy sciences workshop on materials under extreme Environments," U.S. Department of Energy Office of Scientific and Technical Information Report No. 935440 (US DOE - Office of Basic Energy Sciences, 2008).

[2]National Research Council, *Opportunities in High Magnetic Field Science* (National Academies Press, Washington, DC, 2005).
[3]National_Research_Council, *High Magnetic Field Science and Its Application in the United States: Current Status and Future Directions* (National Academies Press, Washington, DC, 2013).
[4]C. Broholm, I. Fisher, J. Moore, M. Murnane, A. Moreo, J. Tranquada, D. Basov, J. Freericks, M. Aronson, A. MacDonald, E. Fradkin, A. Yacoby, N. Samarth, S. Stemmer, L. Horton, J. Horwitz, J. Davenport, M. Graf, J. Krause, M. Pechan, K. Perry, J. Rhyne, A. Schwartz, T. Thiyagarajan, L. Yarris, and K. Runkles, "Basic research needs workshop on quantum materials for energy relevant technology," U.S. DOE Office of Science, Basic Energy Sciences, Office of Scientific and Technical Information Report No. 1616509, 2016.
[5]H. Y. Bai, M. D. Bird, L. D. Cooley, I. R. Dixon, K. L. Kim, D. C. Larbalestier, W. S. Marshall, U. P. Trociewitz, H. W. Weijers, D. V. Abraimov, and G. S. Boebinger, "The 40 T superconducting magnet project at the national high magnetic field laboratory," IEEE Trans. Appl. Supercond. **30**(4), 4300405 (2020).
[6]B. Haberl, D. G. Quirinale, C. W. Li, G. E. Granroth, H. Nojiri, M.-E. Donnelly, S. V. Ushakov, R. Boehler, and B. L. Winn, "Multi-extreme conditions at the second target station," Rev. Sci. Instrum. **93**, 083907 (2022).
[7]I. Remec and F. X. Gallmeier, "Neutronics analyses for the conceptual design of the SNS second target station," J. Neutron Res. **22**(2-3), 265–273 (2020).
[8]J. Hemminger, G. Fleming, and M. Ratner, "Directing matter and energy: Five challenges for science and the imagination," US DOE, Office of Basic Energy Sciences, Office of Scientific and Technical Information Report No. 935427, 2007.
[9]O. Prokhnenko, P. Smeibidl, W.-D. Stein, M. Bartkowiak, and N. Stusser, "HFM/EXED: The high magnetic field facility for neutron scattering at BER II," J. Large-Scale Res. Facil. **3**, 1–7 (2017).
[10]M. Klausz, K. Kanaki, T. Kittelmann, R. Toft-Petersen, J. O. Birk, M. A. Olsen, P. Zagyvai, and R. J. Hall-Wilton, "A simulational study of the indirect-geometry neutron spectrometer BIFROST at the European Spallation Source, from neutron source position to detector position," J. Appl. Crystallogr. **54**, 263–279 (2021).
[11]C. Petrovic, P. G. Pagliuso, M. F. Hundley, R. Movshovich, J. L. Sarrao, J. D. Thompson, Z. Fisk, and P. Monthoux, "Heavy-fermion superconductivity in $CeCoIn_5$ at 2.3 K," J. Phys.: Condens. Matter **13**(17), L337–L342 (2001).
[12]C. S. Yadav and P. L. Paulose, "Upper critical field, lower critical field and critical current density of $FeTe_{0.60}Se_{0.40}$ single crystals," New J. Phys. **11**, 103046 (2009).
[13]B. Ruette, S. Zvyagin, A. P. Pyatakov, A. Bush, J. F. Li, V. I. Belotelov, A. K. Zvezdin, and D. Viehland, "Magnetic-field-induced phase transition in $BiFeO_3$ observed by high-field electron spin resonance: Cycloidal to homogeneous spin order," Phys. Rev. B **69**(6), 064114 (2004).
[14]Y. H. Matsuda, N. Abe, S. Takeyama, H. Kageyama, P. Corboz, A. Honecker, S. R. Manmana, G. R. Foltin, K. P. Schmidt, and F. Mila, "Magnetization of $SrCu_2(BO_3)_2$ in ultrahigh magnetic fields up to 118 T," Phys. Rev. Lett. **111**(13), 137204 (2013).
[15]V. Zapf, M. Jaime, and C. D. Batista, "Bose-Einstein condensation in quantum magnets," Rev. Mod. Phys. **86**(2), 563–614 (2014).
[16]G. Grissonnanche, O. Cyr-Choinière, F. Laliberté, S. René de Cotret, A. Juneau-Fecteau, S. Dufour-Beauséjour, M. È. Delage, D. LeBoeuf, J. Chang, B. J. Ramshaw, D. A. Bonn, W. N. Hardy, R. Liang, S. Adachi, N. E. Hussey, B. Vignolle, C. Proust, M. Sutherland, S. Krämer, J. H. Park, D. Graf, N. Doiron-Leyraud, and L. Taillefer, "Direct measurement of the upper critical field in cuprate superconductors," Nat. Commun. **5**, 3280 (2014).
[17]K. H. Kim, N. Harrison, H. Amitsuka, G. A. Jorge, M. Jaime, and J. A. Mydosh, "Nexus between quantum criticality and phase formation in $U(Ru_{1-x}Rh_x)_2Si_2$," Phys. Rev. Lett. **93**(20), 206402 (2004).
[18]R. Yadav, N. A. Bogdanov, V. M. Katukuri, S. Nishimoto, J. van den Brink, and L. Hozoi, "Kitaev exchange and field-induced quantum spin-liquid states in honeycomb α-$RuCl_3$," Sci. Rep. **6**, 37925 (2016).
[19]B. Haberl, S. Dissanayake, F. Ye, L. L. Daemen, Y. Cheng, C. W. Li, A.-J. Ramirez-Cuesta, M. Matsuda, J. J. Molaison, and R. Boehler, "Wide-angle diamond cell for neutron scattering," High Pressure Res. **37**(4), 495–506 (2017).
[20]B. Haberl, S. Dissanayake, Y. Wu, D. A. A. Myles, A. M. dos Santos, M. Loguillo, G. M. Rucker, D. P. Armitage, M. Cochran, K. M. Andrews, C. Hoffmann, H. Cao, M. Matsuda, F. Meilleur, F. Ye, J. J. Molaison, and R. Boehler, "Next-generation diamond cell and applications to single-crystal neutron diffraction," Rev. Sci. Instrum. **89**(9), 092902 (2018).
[21]A. T. Savici, G. E. Granroth, C. Broholm, Y. S. Lee, and M. D. Bird, "ZEEMANS—A new facility to probe matter at high magnetic field through neutron scattering," in *International Conference on Neutron Scattering* 2009 (IOP Publishing, 2010), p. 251.
[22]B. L. Winn, C. Broholm, M. Bird, B. C. Breneman, M. Coffey, R. I. Cutler, R. C. Duckworth, R. Erwin, S. Hahn, Y. Hernandez, K. W. Herwig, L. D. Holland, K. M. Lonergan, Z. Melhem, S. J. Minter, C. Nelson, M. P. Paranthaman, J. Pierce, J. Ruff, T. shen, T. E. Sherline, P. G. Smeibidl, D. Tennant, D. van der Laan, R. J. Wahle, and Y. Zhang, "Ultra-high field magnets for X-ray and neutron scattering using high temperature superconductors," Oak Ridge National Laboratory Report No. ORNL/TM-2016/712TRN:US1900690, 2017.
[23]J. Y. Jiang, G. Bradford, S. I. Hossain, M. D. Brown, J. Cooper, E. Miller, Y. B. Huang, H. P. Miao, J. A. Parrell, M. White, A. Hunt, S. Sengupta, R. Revur, T. M. Shen, F. Kametani, U. P. Trociewitz, E. E. Hellstrom, and D. C. Larbalestier, "High-performance Bi-2212 round wires made with recent powders," IEEE Trans. Appl. Supercond. **29**(5), 6400405 (2019).
[24]R. Boehler, J. J. Molaison, and B. Haberl, "Novel diamond cells for neutron diffraction using multi-carat CVD anvils," Rev. Sci. Instrum. **88**(8), 083905 (2017).
[25]G. Ehlers, A. A. Podlesnyak, J. L. Niedziela, E. B. Iverson, and P. E. Sokol, "The new cold neutron chopper spectrometer at the spallation neutron source: Design and performance," Rev. Sci. Instrum. **82**(8), 085108 (2011).
[26]G. Ehlers, G. Sala, F. Gallmeier, and K. W. Herwig, "Figure-of-Merit for a cold coupled moderator at the SNS second target station suited for direct geometry inelastic spectrometers," in *22nd Meeting of the International Collaboration on Advanced Neutron Sources (ICANS XXII)* (IOP Publishing, 2018), p. 1021.
[27]F. X. X. Gallmeier and I. Remec, "A liquid hydrogen tube moderator arrangement for SNS second target station," Rev. Sci. Instrum. **93**(8), 083301 (2022).
[28]G. Sala, M. Mourigal, C. Boone, N. P. Butch, A. D. Christianson, O. Delaire, A. J. DeSantis, C. L. Hart, R. P. Hermann, T. Huegle, D. N. Kent, J. Y. Y. Lin, M. D. Lumsden, M. E. Manley, D. G. Quirinale, M. B. Stone, and Y. Z, "CHESS: The future direct geometry spectrometer at the second target station," Rev. Sci. Instrum. **93**(6), 065109 (2022).
[29]I. A. Zaliznyak, A. T. Savici, V. O. Garlea, B. Winn, U. Filges, J. Schneeloch, J. M. Tranquada, G. D. Gu, A. F. Wang, and C. Petrovic, "Polarized neutron scattering on HYSPEC: The HYbrid SPECtrometer at SNS," J. Phys.: Conf. Ser. **862**, 012030 (2017).
[30]O. Kirichek, C. R. Lawson, G. L. Draper, D. M. Jenkins, D. J. Haynes, and S. Lilley, "Solid methane moderators: Thermodynamics and chemistry," J. Neutron Res. **22**(2-3), 281–286 (2020).
[31]M. Bartkowiak, N. Stusser, and O. Prokhnenko, "The design of the inelastic neutron scattering mode for the extreme environment diffractometer with the 26 T high field magnet," Nucl. Instrum. Methods Phys. Res., Sect. A **797**, 121–129 (2015).
[32]W. T. Heller, M. Cuneo, L. Debeer-Schmitt, C. Do, L. L. He, L. Heroux, K. Littrell, S. V. Pingali, S. Qian, C. Stanley, V. S. Urban, B. Wu, and W. Bras, "The suite of small-angle neutron scattering instruments at Oak Ridge National Laboratory," J. Appl. Crystallogr. **51**, 242–248 (2018).
[33]H. R. Wu, Y. Yang, D. S. Hussey, Z. Y. Wang, K. Song, Z. Zhang, Z. S. Wang, Z. Wang, and X. W. Wang, "Study of a nested neutron-focusing supermirror system for small-angle neutron scattering," Nucl. Instrum. Methods Phys. Res., Sect. A **940**, 380–386 (2019).
[34]D. Liu, B. Khaykovich, M. V. Gubarev, J. L. Robertson, L. Crow, B. D. Ramsey, and D. E. Moncton, "Demonstration of a novel focusing small-angle neutron scattering instrument equipped with axisymmetric mirrors," Nat. Commun. **4**, 2556 (2013).
[35]U. B. Hansen, M. Bertelsen, J. Stahn, and K. Lefmann, "An optional focusing SELENE extension to conventional neutron guides: A case study for the ESS

instrument BIFROST," Nucl. Instrum. Methods Phys. Res., Sect. A **852**, 46–56 (2017).
[36]P. K. Willendrup, E. B. Knudsen, E. Klinkby, T. Nielsen, E. Farhi, U. Filges, and K. Lefmann, "New developments in the McStas neutron instrument simulation package," J. Phys.: Conf. Ser. **528**, 012035 (2014).
[37]J. Y. Y. Lin, F. Islam, G. Sala, I. Lumsded, H. Smith, M. Doucet, M. B. Stone, D. L. Abernathy, G. Ehlers, J. F. Ankner, and G. E. Granroth, "Recent developments of MCViNE and its applications at SNS," J. Phys. Commun. **3**(8), 085005 (2019).
[38]O. Arnold, J. C. Bilheux, J. M. Borreguero, A. Buts, S. I. Campbell, L. Chapon, M. Doucet, N. Draper, R. F. Leal, M. A. Gigg, V. E. Lynch, A. Markvardsen, D. J. Mikkelson, R. L. Mikkelson, R. Miller, K. Palmen, P. Parker, G. Passos, T. G. Perring, P. F. Peterson, S. Ren, M. A. Reuter, A. T. Savici, J. W. Taylor, R. J. Taylor, R. Tolchenoy, W. Zhou, and J. Zikoysky, "Mantid-data analysis and visualization package for neutron scattering and mu SR experiments," Nucl. Instrum. Methods Phys. Res., Sect. A **764**, 156–166 (2014).
[39]C. K. Loong, S. Ikeda, and J. M. Carpenter, "The resolution function of a pulsed-source neutron chopper spectrometer," Nucl. Instrum. Methods Phys. Res., Sect. A **260**(2-3), 381–402 (1987).
[40]S. Itoh, T. Yokoo, T. Masuda, H. Yoshizawa, M. Soda, M. Yoshida, T. Hawai, D. Kawana, R. Sugiura, T. Asami, and Y. Ihata, "Improvement for neutron Brillouin scattering experiments on high resolution chopper spectrometer HRC," in *22nd Meeting of the International Collaboration on Advanced Neutron Sources (ICANS XXII)* (IOP Publishing, 2018), p. 1021.